Available online at www.sciencedirect.com

ScienceDirect

Procedia Structural Integrity 44 (2023) 2174–2181

Structural Integrity Procedia

www.elsevier.com/locate/procedia

XIX ANIDIS Conference, Seismic Engineering in Italy

Assessment of the FRCM in-plane behavior in masonry retrofit applications

Michele Angiolilli [a], Amedeo Gregori [b]

[a]*Laboratori Nazionali del Gran Sasso - INFN, Via G. Acitelli 22, L'Aquila 67100, Italy*
[b]*Dipartimento di Ingegneria Civile, Edile e Architettura, Via G. Gronchi 18, Università dell'Aquila, L'Aquila 67100, Italy*

Abstract

Because of its well-documented effectiveness in enhancing the strength and ductility of unreinforced masonry (URM) construction, Fiber Reinforced Mortar (FRCM) is now widely used for the consolidation of heritages, such as churches, palaces, castles, and entirely historical centers. The main purpose of this work is to provide the authors' principal outcomes in the FRCM application to masonry after performing extensive experimental campaigns and numerical simulations over the previous few years. The recent findings have already been appreciated by the research community but have yet to be considered in existing standard codes/recommendations, leaving the contribution of fiber mesh (i) and features of both coating mortar and URM wall (ii) to the improvement of the shear strength of reinforced masonry panels unclear. In fact, unlike FRP, fibers embedded in the mortar coating of the FRCM do not affect the shear strength of the reinforced panel, "limiting" its effect in enhancing the load-bearing capacity of the wall and, therefore, the structure's ductility. This important recent experimental/numerical evidence should be incorporated into the code's recommendation to avoid overestimating the FRCM performance during design phases. Furthermore, the Italian codes suggest simplified amplification factors for estimating the improvement of shear strength owing to the strengthening system that ignores the fact that the greater the thickness of the masonry wall, the lower the FRCM's efficiency, and vice versa. A practice-oriented analytical formulation has been provided to validate such mechanisms by confirming a consistent data set of masonry panels strengthened by FRCM tested under diagonal compression. In this work, a numerical investigation is provided to highlight the importance of considering the effective thickness- and tensile strength-ratio between the FRCM mortar coating and the URM panel to accurately predict the enhancement in the mechanical behaviour of the FRCM-reinforced masonry.

Keywords: Unreinforced Masonry Structures, Seismic Vulnerability, Stone Masonry, Fiber Reinforcement, Cultural Heritage, Diagonal Compression Test, Shear Strength

10.1016/j.prostr.2023.01.278

1. Introduction

The high vulnerability of most UnReinforced Masonry (URM) architectural and artistic heritages has been highlighted during recent seismic activity, namely the 2009-2012-2016 Italian earthquakes (see Augenti and Parisi 2010, D'Ayala and Paganoni 2011, Penna 2014, Sorrentino 2019). Among the different masonry typologies, the irregular stone URM has been confirmed to be characterized by the highest vulnerability class, as also defined by Grünthal et al. (1998) in the European Macroseismic Scale EMS98 and supported by several studies (e.g. Rezaie, et al. (2020), Senaldi et al. (2020), Cattari et al. 2022). In fact, most constructions composed of irregular stone URM collapsed completely or partially during seismic events owing to the complete loss of cohesion between the stones and the brittle collapse of the structure that results (i.e. local mechanisms, see Angiolilli et al. (2022)). That behaviour can also be negatively influenced by the panel-size effect, as evidenced in Angiolilli et al. (2021a), in which it was found that real panels, which are much larger than 1 m - 1.5 m typical of experimental samples, may tend to almost brittle behavior due to size-effect, a phenomenon inherently associated with quasi-brittle materials, which depends on the evolution of the fracture process zone as well as the minimum crack length developed during failure.

When local mechanisms are prevented (by transverse elements, the good interlock of rigid floors, and the absence of thrusting/heavy roof systems), the overall response of historic URM is governed by the in-plane damage that occurs to piers (i.e., vertical resistant elements) and/or spandrels (i.e., parts of walls between two vertically aligned openings) (see Lagomarsino et al. (2022)). In order to improve the in-plane (as well as the out-of-plane) capacity with minimal increases in mass and stiffness of the structures, as well as to ensure greater compatibility with the original materials of the existing/historical buildings, fiber-based retrofitting techniques have been developed. In the last years, Fiber Reinforced Cementitious Matrix (FRCM) has been increasingly considered for strengthening and repair of both modern and historic URM also due to the well-known disadvantages of Fiber Reinforced Polymers (FRP) applied to irregular URM (e.g. Kouris and Triantafillou (2018)) or other traditional systems.

In the current literature, most of the experimental tests on the FRCM system were performed on regular brick/tuff/concrete masonry (e.g. Del Zoppo et al. (2019)). A collection of experimental tests on FRCM-reinforced irregular stone URM can be found in Angiolilli et al. (2021b). In Gattesco and Boem (2015), specimens strengthened with various percentages of reinforcement showed no noticeable variations in their tensile strength (and shear modulus), whereas fiber mesh plays a significant role in enhancing the post-peak behavior of reinforced masonry (RM) by providing tensile resistance after the material cracks due to stress redistribution and enabling the masonry to attain substantial values of the deformation capacity. The same trend was numerically supported by Angiolilli et al. (2020a, 2021c), who demonstrated that fibers primarily serve to carry tensile stresses (load-bearing capacity) and redistribute stress on masonry panels, while the thickness and mechanical characteristics of the reinforcing mortar have a significant impact on the shear strength of RM panels.

Recent research has studied the use of short fibers embedded in lime mortar matrix (see Abbass et al. (2020), Angiolilli et al. (2020b), Del Zoppo et al. (2020), Vailati et al. (2021)) as an alternate reinforcing technique for existing masonry to get around the restrictions of both FRP and FRCM regarding the orientation of the fibers in certain directions. However, further investigation is still required.

The mechanical behavior of FRCM applied to URM has been the subject of extensive investigation over the past 10 years. The most recent results, however, are still not considered by the existing standard codes. In order to provide a better understanding of the factors affecting the mechanical behavior and damage evolution of stone URM panels reinforced by FRCM, the main experimental and numerical aspects investigated in previous research performed by the Authors (e.g. Angiolilli et al. 2020a, 2021b, 2021c) are discussed in this work, specifically the thickness of the reinforcement, the bond behavior at the FRCM-masonry interface, and the role of fiber grids in the strengthening system. Additionally, all the collected data (60 tests) was used to support a straightforward analytical equation for estimating the shear strength of the RM based on a few characteristics of the unreinforced masonry and the FRCM mortar.

Nomenclature

RM	Reinforced masonry (i.e. URM coated by FRCM)
URM	Unreinforced masonry

n_f	Total number of FRCM layers
$f_{c,URM}$	Compressive strength of the URM
$f_{c,extURM}$ $f_{c,intURM}$	Compressive strength of external leaves or internal core of a the three-leaf URM
f_{ctm}^	Tensile strength of the FRCM matrix
t_{FRCM}	Thickness of the single FRCM layer
t_{RM} , t_{URM}	Thickness of the RM (i.e. $t_{URM} + n_f t_{FRCM}$) or that of the URM
V_{ext}/V_{tot}	Volumetric ratios of external layers of a three-leaf URM
V_{int}/V_{tot}	Volumetric ratios of the core of a three-leaf URM
β	FRCM efficiency coefficient (i.e. $\tau_{0,RM} / \tau_{0,URM}$)
λ_b	Corrective coefficient for the computation of β
λ_{ext} , λ_{int}	Corrective coefficients for external leaves or internal core of a the three-leaf URM
$\tau_{0,RM}$, $\tau_{0,URM}$	Tensile strength of RM or URM, respectively

2. Brief description of the experimental tests described in the current literature

The outcomes of other research studies on stone URM panels with single and/or multiple leaf cross sections that were enhanced by FRCM are summarized in the current section. They only included tests that used the diagonal compression setup. The benchmark results (19 URMs and 41 RMs, for a total of sixty tests) are presented in detail in Angiolilli et al. (2020a, 2021b), Corradi et al. (2014), Gattesco and Boem (2015), Gattesco et al. (2015a, 2015b), Del Zoppo et al. (2020), Balsamo et al. (2014), and partially reported here. The following labels are used to present the results: S1,.. L1,… The first index identifies the test type (S = on-site; L = lab-test); the second index is the panel's progressive number. Then the indexes URM or RM were adopted for unreinforced and reinforced masonry, respectively.

Results from testing on masonry panels constructed in the lab using stone components recovered from the rubble of the Margherita Palace (L'Aquila, Italy) - which is representative of existing URM buildings in the areas of the central Apennines - following the 2009 earthquake are specifically addressed in Angiolilli et al. (2020a). For the production of the specimens, the same construction method used in the historic structure was used. Stone components with a typical average size of around 0.15 m were utilized. By combining commercial Natural Hydraulic Lime (NHL) mortar, local crushed limestone sand, and local natural clay in a ratio of 1:2:1, the original mortar characteristics were replicated. This resulted in a mortar with extremely friable behavior and low compressive strength of around 2 MPa. All of the wall specimens had a 15-month curing process, allowing the lime-based mortar to harden at room conditions. Two of the six specimens were kept unreinforced while the remaining four were strengthened by FRCM. Four glass fiber anchors were used. Moreover, the laboratory panels were tested under in-plane monotonic loading. These tests are labelled as L1.

Results of on-site experiments on stone masonry panels separated from the walls of the Margherita Palace are documented in Angiolilli et al. (2021b). In order to give a reference value for the unreinforced masonry, only two of the four panels were strengthened using FRCM. The FRCM was made up of carbon shear connections and a glass-fiber grid that was encased in an NHL-based mortar and coated over the brick surfaces. These tests have the label S1.

Results from on-site testing on four panels, each 0.48 m to 0.57 m thick and isolated from a historic building in Umbria (Italy), as well as five tests on stone-wall panels of a historic building in L'Aquila built of double-leaf walls, were published in Corradi et al. (2014). The number of tests is higher than that of the panels because the samples that had been examined in their original condition were repaired before being retested. Glass-FRCM 30 mm tick and five connections made of two unidirectional fiberglass L-shaped bars constitute the strengthening system. These tests have the S2 label.

Results of several masonry types reinforced by FRP with diverse characteristics were reported in Gattesco and Boem (2015). Only masonry made of rubble stone was considered in this study. The walls had a cross-sectional thickness of 0.40 m and 0.70 m and were constructed in the lab. The strengthening method involved applying a glass-FRCM layer with a thickness of between 30 and 45 mm to both faces of the structure, as well as inserting five L-shaped glass-FRP connectors through the thickness of the walls. These tests employ the L2 labels.

A total of twelve experiments on rubble stone masonry samples (4 URMs and 8 RMs) with a thickness of 0.4 m were taken into consideration from the extensive experimental campaign described in Gattesco et al. (2015a). Two different types of poor infill mortar that are frequently used in the two-leaf brickwork of old structures were used to construct the panels in a laboratory. The glass FRP reinforcement system included six L-shaped glass-FRP connectors and glass FRP meshes with various characteristics embedded in a 30 mm thick mortar coating. These tests have the label L3.

Two tests (1URM and 1RM) were considered by Gattesco et al. (2015b). A further test from the same research program that used a hybrid reinforcement was not considered (reticolatus and glass-FRCM). The thickness of the double leaf rubble masonry was 0.40 m. Six L-shaped glass-FRP connectors and 30 mm thick glass-FRCM made up the reinforcement. L4 is the test label.

Nine experiments (3 URMs and 6 RMs) from the broad experimental campaign described in Del Zoppo et al. (2020) were taken into consideration. Other tests regarding strengthening systems that consisted of short-fibers embedded in the mortar matrix (instead of the typical fiber grid) were not taken into account, since further research is needed to determine whether the fiber grid affects the improvement of shear strength. Only one side of the half of the RM specimens had reinforcement. For all the specimens, no anchors were used. Tests have the label L5.

Finally, five tests (1 URM and 4 RMs) were considered by Balsamo et al. (2014). In that research, limestone masonry panels were built aiming to reproduce the typical existing building in the area of L'Aquila (Italy). Both basalt-FRCM and glass-FRCM were adopted without using connectors. Tests are labeled as L6.

Definitely, from the sixty collected tests (19 URMs and 41 RMs), one can compute the mean value of $\tau_{0,RM}$ and $\tau_{0,URM}$ (according to RILEM (1994)) equal to 0.379 MPa (CoV=0.315) and 0.143 MPa (CoV=0.596), respectively. The mean value of the reinforcement efficiency, given by the ratio between the mean strength value of the RM and URM of each experimental campaign (i.e. $\tau_{0,RM}$ / $\tau_{0,URMm}$), is 3.27 (CoV=0.671). In particular, for each experimental campaign, one can compute the mean shear strength of the URM panel (i.e. $\tau_{0,URMm}$). Then, the shear strength of each reinforced panel ($\tau_{0,RM}$) is divided by the respective τ0,URMm. The reinforcement efficiency computed for each experimental campaign is reported in Fig.1.

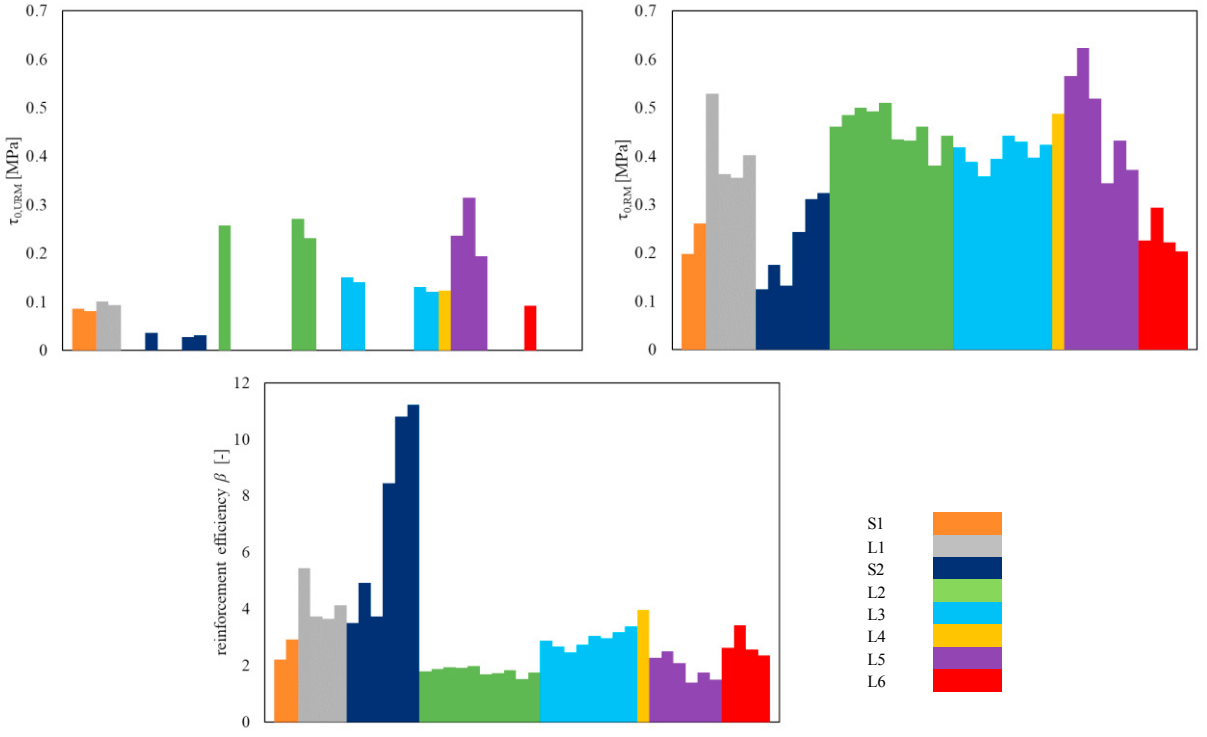

Fig. 1. Results expressed in terms of shear strengths $\tau_{0,URM}$ and $\tau_{0,RM}$ and the FRCM efficiency β collected for 19 URMs and 41 RMs

In general, one can see that the higher β (i.e. more than 10) is associated with the case characterized by the lower shear strength of the URM panels, namely the S2 case. On the contrary, the lower β (i.e. 1.4) is associated with the case characterized by the higher shear strength of the RM panels, namely the L5 case. This initial tendency may be crucial to begin to comprehend the physics underlying the complex behavior of URM reinforced by FRCM.

Furthermore, from Fig.1, one can see that the β values estimated by the experimental campaigns were much higher as compared with the ones suggested by Standard Codes. In particular, the CNR-DT 215 (2018) and MIT (2019) propose β equal to 1.5 or 2.5, respectively for irregular stone masonry walls reinforced by FRCM. Note that MIT (2019) concerns, more generally, reinforced coating and not particularly about FRCM. Moreover, observing Tab.1, one can see that β values proposed by MIT (2019) tend to be higher for masonry types characterized by lower quality. The same trend cannot be observed instead for the β values proposed by CNR-DT 215 (2018). This first analysis shows that the present standard codes also exhibit a lack of understanding of the mechanical behavior of FRCM-reinforced URM.

Table 1. FRCM efficiency coefficients (β) proposed in the Codes for different URM type

URM type	CNR-DT 215 (2018)	MIT (2019)
Masonry in disorganized stones (pebbles, or erratic/irregular stones)	1.5	2.5
Masonry in rough-hewn stone, with faces of inhomogeneous thickness	1.5	2
Masonry in split stones, well laid	2	1.5
Masonry in soft stone (tuff, macco, etc.)	2	1.5-1.7
Masonry in squared stony blocks	1.2	1.2
Masonry in bricks and lime mortar	1.7	1.5
Masonry in half-full bricks with cement mortar	1.3	1.3

Apart from the initial mechanical properties of the URM panel (partially taken into account by standard codes although with questionable values, as commented above), the reinforcement efficiency also depends on the thickness ratio between the URM panel and the FRCM mortar coating (Angiolilli et al. (2020b, 2021c)); the FRCM effectiveness in terms of shear strength decreases with increasing masonry wall thickness, and vice versa, whereas it decreases with decreasing FRCM mortar coating thickness, and vice versa. Note that the thickness ratio is not considered within standard codes. Although this aspect may have a secondary importance regarding thickness of FRCM matrix because it varies between a prefixed range (i.e. 5 mm to15 mm), note that that value excludes the levelling of the substrate. For irregular substrate, typical of stone URM, the effective thickness of FRCM matrix is much higher. On the other hand, the thickness of the walls in existing URM buildings varies widely, also between the different floor levels of the same building. Hence, the URM/FRCM thicknesses are important factors to be considered in the β prediction.

Last but not least, another discrepancy between experimental evidence and standard specifications concerns how fiber mesh, which is embedded in the FRCM matrix, affects the shear strength of RM. In fact, in ACI 549.4R (2013) and CNR-DT 215 (2018), the shear strength of RM is computed as the sum of the URM's nominal shear strength and the FRCM contribution, with the latter being specified to depend also on the area of the fabric reinforcement by unit width. However, despite the various mesh areas, space grids, and materials (such as glass, carbon, etc.), no noticeable shear strength difference can be shown as a function of those features (Gattesco and Boem (2015) and Angiolilli et al. (2020a, 2021c)). Those characteristics, instead, affect largely the ductility of the RM. The formulation provided in ACI 549.4R, then reported also in CNR-DT 215, was based on experimental tests performed on clay brick masonry reinforced by (i) near-surface mounted (NSM) glass FRP bars externally bonded, (ii) glass/carbon FRP laminates, and (iii) glass FRP grid reinforced polyurea (see Babaeidarabad et al. (2014)). Hence, that formulation was initially developed for FRPs and subsequently extended to FRCM on the (wrong) assumption that these systems' mechanical behavior is comparable.

3. Analytical interpretation of the data

The collected data allowed for the individuation of an analytical relation to estimate the RM strength. The behavior of URM coupled with FRCM can be substantially compared to the behavior of three-leaf masonry under compression that is described in Penelis and Penelis (2020). In fact, with the three-leaf URM, the outermost leaves' mechanical properties are much higher than the core. As a result, a greater portion of the applied load is carried by the exterior leaves. Here, it may be assumed that the three-leaf URM's interior infill and exterior leaves are, respectively, the FRCM layer and the single URM, as the FRCM coating carries the greater percentage of the load with respect to URM wall.

$$f_{c,URM} = \lambda_{ext} \frac{V_{ext}}{V_{tot}} f_{c,ext,URM} + \lambda_{int} \frac{V_{int}}{V_{tot}} f_{c,int,URM} \tag{1}$$

where V_{ext}/V_{tot} (and V_{int}/V_{int}) is the volumetric ratios of external layers (or infill). Note that the original formulation of (1) also considers corrective factors, which take into account of the mutual interaction between the external layers and the core; λ_{ext} must be higher than 1 as the core is confined by the external leaves while λ_{int} must be less than 1 as the external leaves are subjected to thrust actions by the core due to its dilatancy. In Tassios (2004), λ_{int} or λ_{ext} were analytically defined. Anyhow, in this work, they can be assumed equal to 1. Therefore, Eq. (1) may be rewritten as Eq. (2) to predict the RM shear strength, by assuming the same law applied for the compression strength as well as substituting the exterior leaves and core of the three-leaf URM with the FRCM layer and URM wall, respectively:

$$\tau_{0,RM} = \frac{V_{URM}}{V_{tot}} \tau_{0,URM} + \frac{V_{FRCM}}{V_{tot}} f_{tcm^\wedge} \tag{2}$$

Note that, in Eq. (1), the shear strength of the FRCM can be assumed equal to that of the FRCM matrix (here defined as $f_{tcm^\wedge}$) due to the negligible effect provided by the mesh in enhancing the shear strength of the FRCM applied to URM (Angiolilli et al. (2021c)). Moreover, since $V_{tot} = V_{URM} + n_f V_{FRCM}$, and the surface area of both the URM and FCRM is the same (equal to almost 1.2 m×1.2 m for the analyzed cases), one can simplify Eq. (2) as follows:

$$\tau_{0,RM} = \frac{t_{URM}}{t_{URM} + n_f t_{FRCM}} \tau_{0,URM} + \frac{n_f t_{FRCM}}{t_{URM} + n_f t_{FRCM}} f_{tcm^\wedge} \tag{3}$$

Definitively, assuming $t_{URM} + n_f t_{FRCM} = t_{RM}$, Eq. (3) can be simplified as:

$$\tau_{0,RM} = \lambda_b \frac{t_{URM} \tau_{0,URM} + n_f t_{FRCM} f_{tcm^\wedge}}{t_{RM}} \tag{4}$$

Note that in Eq. (4), a corrective factor λ_b was introduced to consider the effect of the bond behavior at the FRCM-URM interface. Indeed, simulations performed by Angiolilli (2020a) showed that the shear strength increases of about 10% by assuming high bond behavior instead of weak bond). In that study, the interface between stone particles and reinforcement mortar particles was simplistically assumed to be flat. For irregular stone masonry, it is presumable that the effect of the bond behavior could be even higher than 20% because of the interlocking effect. Furthermore, λ_b in Eq. (4) also considers the large variability of the mechanical and geometrical properties. In particular, the exact estimation of the thicknesses of the coating mortar is difficult to perform because of the irregularity of the stone masonry surface. The thickness of the mortar coating is measured excluding the levelling of the substrate (see CNR-DT 215 (2018)) tending to underestimate the actual equivalent thickness applied to the masonry surface. Hence, for the reasons described above, λ_b should be plausibly higher than 1. In Angiolilli et al. (2021b) the mean value of λ_b for all the collected data was 1.29. Assuming that value for λ_b and for all the collected data, it is possible to see a comparison between the experimental $\tau_{0,RM}$ and the ones predicted by Eq. (4) (blue markers of Fig. 2) showing a very good match (R-squared of 0.96). The reliability of Eq. (4) is also confirmed by the results of the numerical simulations performed by Angiolilli et al. (2020a, 2021a, 2021c) through a sophisticated numerical framework, based on the Lattice Discrete Particle Model – LDPM (see also Mercuri et al. (2020, 2021)). Indeed, the red markers of Fig. 2 are

associated with the shear strength simulated by LDPM varying different mechanical/geometrical properties of both the URM and FRCM. Note that for the simulations, λ_b=1.1, which is only associated to the bond behavior at the FRCM-URM interface; The simulations perfectly match the results of Eq. (4) (R-squared of about 1).

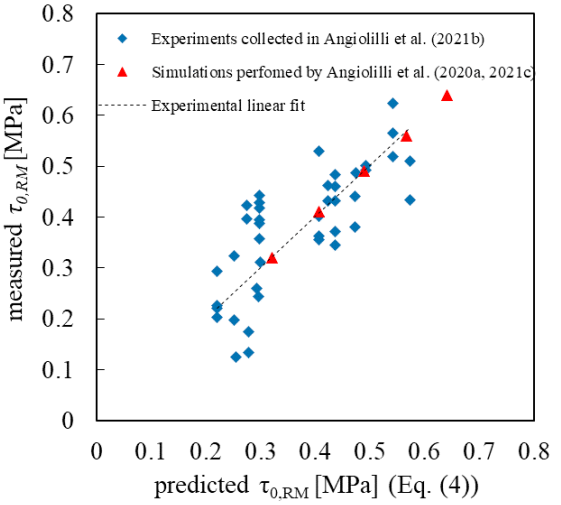

Fig. 2. Measured Vs predicted shear strength of the FRCM-reinforced masonry.

From Eq. (4) it is easy to estimate the FRCM efficiency coefficient β (i.e. $\tau_{0,RM}/\tau_{0,URM}$) trough Eq. (5) to estimate the shear strength of the RM note that of the URM, tensile strength of the FRCM matrix and the relative thicknesses.

$$\beta = \lambda_b \frac{t_{URM}\,\tau_{0,URM} + n_f\,t_{FRCM}\,f_{tcm^\wedge}}{t_{RM}\,\tau_{0,URM}} = \lambda_b \left[1 + \frac{n_f\,t_{FRCM}}{t_{RM}} \left(\frac{f_{tcm^\wedge}}{\tau_{0,URM}} - 1\right)\right] \tag{5}$$

4. Conclusions

The present work investigated the results of experimental campaigns present in the current literature to highlight some deficiencies in current standard codes in estimating the ultimate shear strength of URM strengthened by FRCM. In particular, only the results of stone walls, with single and/or multi-leaf cross sections, tested under diagonal compression were considered in this work, being the most diffused masonry typology within Italian residential building stock. First, it was pointed out that the effective enhancement of FRCM may be severely underestimated by the reinforcement efficiency coefficients indicated by standard codes. Although this might be seen as a precautionary measure to avoid overly depending on the mechanical property enhancements offered by reinforcing systems in the verification/design phase of existing masonry buildings, it could have the unintended consequence of completely miscalculating the seismic performance of FRCM-strengthened structures. The results of this study, in fact, give insight into the effect of the mechanical and geometric properties of both URM and FRCM on the ultimate shear strength of the reinforced masonry. In existing URM buildings, it is common to notice a spatial randomness of material properties as well as variations in the masonry thickness, especially between the different floor levels. Therefore, the reinforcement efficiency coefficient needs to be calibrated appropriately based on such kinds of variables. To this end, a comprehensive set of tests taken from recent literature as well as simulations carried out by an advanced numerical framework have been used to validate an analytical formulation. The excellent match promotes the adoption of the proposed formulation to predict the performance of FRCM-strengthened masonry more accurately.

References

Abbass, A., Lourenço, P. B., Oliveira, D. V. , 2020. The use of natural fibers in repairing and strengthening of cultural heritage buildings. Materials Today: Proceedings, 31, S321-S328.

ACI 549.4R, 2013, Guide to design and construction of externally bonded fabric-reinforced cementitious matrix (frcm) systems for repair and strengthening concrete and masonry structures, Technical Document.

Angiolilli, M., Gregori, A., Pathirage, M., Cusatis, G., 2020a. Fiber Reinforced Cementitious Matrix (FRCM) for strengthening historical stone masonry structures: Experiments and computations. Engineering Structures, 224, 111102.

Angiolilli, M., Gregori, A., Vailati, M., 2020b. Lime-based mortar reinforced by randomly oriented short fibers for the retrofitting of the historical masonry structure. Materials, 13(16), 3462.

Angiolilli, M., Pathirage, M., Gregori, A., Cusatis, G., 2021a. Lattice discrete particle model for the simulation of irregular stone masonry. Journal of Structural Engineering, 147(9), 04021123.

Angiolilli, M., Gregori, A., Cattari, S., 2021b. Performance of Fiber Reinforced Mortar coating for irregular stone masonry: Experimental and analytical investigations. Construction and Building Materials, 294, 123508.

Angiolilli, M., Gregori, A., Cusatis, G., 2021c. Simulating the Nonlinear Mechanical Behavior of FRCM-strengthened Irregular Stone Masonry Walls. International Journal of Architectural Heritage, 1-17.

Angiolilli, M., Brunelli, A., Cattari, S., 2022. Fragility curves of masonry buildings in aggregate accounting for local mechanisms and site effects, submitted to Bull. Earth. Eng. doi:10.21203/rs.3.rs-1700540/v1

Augenti, N., Parisi, F., 2010. Learning from construction failures due to the 2009 L'Aquila, Italy, earthq. J. Perform. Constr. Facil., 24(6), 536-555.

Balsamo, A., Iovinella, I., Morandini, G., 2014, March. FRG strengthening systems for masonry building. In NZSEE conference.

Babaeidarabad, S., De Caso, F., Nanni, A. (2014). URM walls strengthened with fabric-reinforced cementitious matrix composite subjected to diagonal compression. Journal of Composites for Construction, 18(2), 04013045.

Cattari, S., Angiolilli, M., Alfano, S., Brunelli, A., De Silva, F., 2022. Investigating the combined role of the structural vulnerability and site effects on the seismic response of a URM school hit by the Central Italy 2016 earthquake. Structures (Vol. 40, pp. 386-402).

CNR-DT 215, 2018. National Research Council. Guide for the design and construction of externally bonded fibre reinforced inorganic matrix systems for strengthening existing structures. Rome, 06.02.2019; version of June 30, 2020.

Corradi, M., Borri, A., Castori, G., Sisti, R., 2014. Shear strengthening of wall panels through jacketing with cement mortar reinforced by GFRP grids. Composites Part B: Engineering, 64, 33-42.

D'Ayala, D. F., Paganoni, S., 2011. Assessment and analysis of damage in L'Aquila historic city centre after 6th April 2009. Bulletin of Earthquake Engineering, 9(1), 81-104.

Del Zoppo, M., Di Ludovico, M., Prota, A., 2019. Analysis of FRCM and CRM parameters for the in-plane shear strengthening of different URM types. Composites Part B: Engineering, 171, 20-33.

Del Zoppo, M., Di Ludovico, M., Balsamo, A., Prota, A., 2020. Diagonal compression testing of masonry panels with irregular texture strengthened with inorganic composites. Materials and Structures, 53(4), 1-17.

Gattesco, N., Boem, I., 2015. Experimental and analytical study to evaluate the effectiveness of an in-plane reinforcement for masonry walls using GFRP meshes. Construction and Building Materials, 88, 94-104.

Gattesco, N., Boem, I., Dudine, A., 2015a. Diagonal compression tests on masonry walls strengthened with a GFRP mesh reinforced mortar coating. Bulletin of Earthquake Engineering, 13(6), 1703-1726.

Gattesco, N., Amadio, C., Bedon, C. 2015b. Experimental and numerical study on the shear behavior of stone masonry walls strengthened with GFRP reinforced mortar coating and steel-cord reinforced repointing. Engineering Structures, 90, 143-157.

Grünthal, G., Musson, R., Schwarz, J., Stucchi, M., 1998. European Macroseismic Scale 1998. Cahiers de Centre Européen de Géodynamique et de Seismologie, Volume 15 (1998), Luxembourg

Kouris, L. A. S., Triantafillou, T. C., 2018. State-of-the-art on strengthening of masonry structures with textile reinforced mortar (TRM). Construction and Building Materials, 188, 1221-1233.

Lagomarsino, S., Cattari, S., Angiolilli, M., Bracchi, S., Rota, M., Penna, A. 2022. Modelling and Seismic Response Analysis of Existing URM Structures. Part 2: Archetypes of Italian Historical Buildings. Journal of Earthquake Engineering, 1-26.

Mercuri, M., Pathirage, M., Gregori, A., Cusatis, G. 2020. Computational modeling of the out-of-plane behavior of unreinforced irregular masonry. Engineering Structures, 223, 111181.

Mercuri, M., Pathirage, M., Gregori, A., & Cusatis, G. 2021. On the collapse of the masonry Medici tower: An integrated discrete-analytical approach. Engineering Structures, 246, 113046.

MIT2019, Ministry of infrastructures and transportation, circ. c.s.ll. pp. no. 7 of 21/1/2019, Ministerial Decree DM; , in italian.

NTC, Norme tecniche per le costruzioni in zone sismiche, in Italian, Ministerial Decree DM; 2018.

Penelis, G. G., and Penelis, G. G. (2020). Structural restoration of masonry monuments: arches, domes and walls. CRC Press.

Penna, A., Morandi, P., Rota, M., Manzini, C. F., Da Porto, F., Magenes, G., 2014. Performance of masonry buildings during the Emilia 2012 earthquake. Bulletin of Earthquake Engineering, 12(5), 2255-2273.

Rezaie, A., Godio, M., Beyer, K., 2020. Experimental investigation of strength, stiffness and drift capacity of rubble stone masonry walls. Construction and Building Materials, 251, 118972.

Rilem, (1994). LUM B6 Diagonal tensile strength tests of small wall specimens, 488-489.

Senaldi, I. E., Guerrini, G., Comini, P., Graziotti, F., Penna, A., Beyer, K., Magenes, G. 2020. Experimental seismic performance of a half-scale stone masonry building aggregate. Bulletin of Earthquake Engineering, 18(2), 609-643.

Sorrentino, L., Cattari, S., Da Porto, F., Magenes, G., & Penna, A. (2019). Seismic behaviour of ordinary masonry buildings during the 2016 central Italy earthquakes. Bulletin of Earthquake Engineering, 17(10), 5583-5607.

Tassios, T. P. (2004). Rehabilitation of three-leaf masonry. Evoluzione nella sperimentazione per le costruzioni, Seminario Internazionale, 26.

Vailati, M., Mercuri, M., Angiolilli, M., Gregori, A., 2021. Natural-Fibrous Lime-Based Mortar for the Rapid Retrofitting of Heritage Masonry Buildings. Fibers, 9(11), 68.